ISSN: 0067-2904

Electrochemical Synthesis of Fe-doped TiO_2 Nanotube for Gas Sensor Application

Mina Mohammed Faris[1], Asmaa Kadim Ayal[2*]
[1]*Department of Chemistry, College of Science, University of Baghdad, Baghdad, Iraq*
[2]*Department of Chemistry, College of Science for Women, University of Baghdad, Baghdad, Iraq*

Received: 10/10/2023 Accepted: 6/5/2024 Published: 30/4/2025

Abstract

Titanium dioxide (TiO_2) nanotubes have gained particular interest as a material for gas sensors because of their vertical arrays, prepared by the anodization procedure. The presence of several oxygen vacancies in these nanotubes facilitates gas diffusion and provides additional active sites. This study examined the impact of voltages on the process of depositing iron nanoparticles onto arrays of TiO_2 nanotubes (TNTs) for use as a gas sensor. The TNTs are manufactured using a straightforward and economical electrochemical anodization technique, specifically for gas sensor applications. By varying the deposition voltage (2-6 volts), ordered Fe-TNTs were efficiently manufactured using a simple two-step electrochemical process. It utilized energy-dispersive X-ray spectroscopy (EDX), X-ray diffraction (XRD), and field-emission scanning electron microscopy (FESEM) to study morphology, structure, and composition. Furthermore, gas sensor testing was implemented to examine the gas sensor's response. An increase in the Fe doping voltage with TNTs altered the structure of the nanotubes, particularly at the highest voltages, according to XRD analysis. The best sensor for Fe-TNTs was made by doping Fe with TiO_2 nanotubes at a doping voltage of 3 volts, depending on how well the gas sensitizers worked. The study demonstrated that using iron can increase TiO_2's efficiency as a gas sensor.

Keywords: Electrochemical synthesis, hydrogen sulfide, Fe-TNTs, sensitivity, TiO_2 nanotubes.

تحضير الانابيب النانوية TiO_2 المشوبة مع الحديد لتطبيق مستشعر الغاز

مينا محمد فارس[1], اسماء كاظم عيال[2*]
[1]قسم الكيمياء, كلية العلوم, جامعة بغداد, بغداد, العراق
[2] قسم الكيمياء, كلية العلوم للبنات, جامعة بغداد, بغداد, العراق

الخلاصة

اكتسبت الأنابيب النانوية لثاني اوكسيد التيتانيوم (TiO_2) اهتمام خاصاً كمادة لأجهزة استشعار الغاز بسبب مصفوفاتها العمودية, التي تم تحضيرها بواسطة اجراء الاكسدة. ان وجود العديد من شواغر الأوكسجين في هذه الأنابيب النانوية يسهل انتشار الغاز و يوفر مواقع نشطة اضافية. تناولت هذه الدراسة تأثير الفولتية على عملية ترسيب دقائق الحديد النانوية على مصفوفات الأنابيب النانوية TiO_2 (TNTs) لاستخدامها كجهاز استشعار للغاز. تم تصنيع TNTs باستخدام تقنية أنودة كهروكيميائية مباشرة واقتصادية، خصيصًا لتطبيقات مستشعرات

*Email: asmaakaachem@csw.uobaghdad.edu.iq

الغاز. من خلال تغيير جهد الترسيب (2−6 فولت)، تم تصنيع Fe−TNT المطلوبة بكفاءة باستخدام عملية كهروكيميائية بسيطة من خطوتين. تم استخدام التحليل الطيفي لتشتت الطاقة (EDX)، و حيود الأشعة السينية (XRD)، و المجهر الإلكتروني الماسح (FESEM) لدراسة الشكل و البنية والتركيب. علاوة على ذلك، تم إجراء اختبار مستشعر الغاز لفحص استجابة مستشعر الغاز. أدت الزيادة في فولتية تشويب TNTs مع الحديد إلى تغيير بنية الأنابيب النانوية، خاصة عند أعلى الفولتيات، وفقًا لتحليل XRD. تم تصنيع أفضل مستشعر لـ Fe−TNTs عن طريق تشويب أنابيب TiO_2 النانوية بالحديد عند فولتية تشويب قدرها 3 فولت، اعتمادًا على مدى جودة عمل متحسس الغاز. أظهرت الدراسة أن استخدام الحديد يمكن أن يزيد من كفاءة TiO_2 كجهاز استشعار للغاز.

1. Introduction

Hydrogen sulfide (H_2S) is generated by various sources, including hot springs, natural gas, crude petroleum, and organic pollutants found in effluent and waste [1]. Even at low concentrations of H_2S, this gas can have severe effects on humans' respiratory and nervous systems. TiO_2 has been recently gaining attention due to its low cost [2], eco-friendliness [3], chemical stability as a catalyst [4], and potential as a gas sensor [5,6]. Moreover, it allows for easily adjustable surfaces and structural features [7,8]. Notwithstanding numerous endeavors, augmenting the sensitivity of H_2S gas detection continues to be a significant obstacle. In recent times, greater importance has been placed on monitoring the air and environment quality [9,10], along with detecting war gases and explosives by evaluating their vapors [11,12]. In 2005, the Kyoto Protocol came into force to limit some gas emissions, including H_2S that led to global warming [13]. Diverse industries, including medical diagnostics, the chemical industry, and the food industry, rely heavily on sensitive gas sensors for monitoring and detecting gases. These sensors must be capable of detecting low concentrations at the level of single parts per million (ppm) or even parts per billion (ppb) in the atmosphere of air [14-16]. For many years, photo- and electrochemical systems (such as photocatalysis [17] and solar cells [18]) have used titanium dioxide (TiO_2). Researchers have attempted to use TiO_2 for detecting various gases such as NH_3 [19], CO [20], H_2 [21], H_2S [22], alcohol vapors [23], humidity [24], and others. TiO_2 has a wide range of possible uses in a variety of industries today, including photocatalysis, optoelectronics, piezoelectricity, acoustoelectric, and water splitting for the production of hydrogen [25]. The field of gas sensors most commonly employs resistance sensors. These work by altering a semiconductor's electrical conductance because atoms and molecules adhere to its surface [26]. Semiconductors with a broad energy range provide excellent measuring potential in resistance sensors because the right doping can change their sensory characteristics. UV light triggers this particular type of gas sensor, which operates at an increased temperature, typically ranging from 200 to 400 °C [27]. In addition, existing studies show several methods for preparing H_2S gas sensors. For example, Ag-doped TiO_2 nanofibers were prepared using an electrospinning technique [28], while CuO-doped TiO_2 nanoparticles were fabricated using a sol-gel method [29]. In this work, we will attempt to offer a simple electrodeposition method to fabricate Fe-TNTs as a gas sensor. Our research revolves around comparing and examining the influence of the voltage on the structure and the sensitivity for detecting hazardous gases (H_2S) at room temperature of the prepared gas sensors.

2. Experimental

2.1. Materials and methods

A simple two-step electrochemical procedure was employed to synthesize Fe-TNTs. TNTs were first made by anodization [30]. Titanium foil samples (10 mm × 20 mm, 99.5% purity, Sigma Aldrich) were cleaned using ultrasonication in three different solvents for a total of 15 minutes: acetone, isopropanol, and deionized water. Following this, titanium underwent anodization in a typical two-electrode cell, utilizing high-density graphite as the cathode and Ti

foil as the anode. Anodization was performed in a mixture of electrolytes, which was prepared by mixing ethylene glycol 190 mL, 10 mL DI water, and 0.5 wt.% NH_4F at 30 volts for 1 hour. After anodization, the as-formed samples were rinsed with deionized water and subsequently dried in air, followed by calcination in air at 500 ^oC for 1 hour. The calcination process is crucial to induced crystallinity in titania nanotubes (TNTs) [31]. The electrodeposition method then used the previously prepared TNTs as a substrate, sensitizing them to iron. The electrodeposition of iron in a two-electrode cell was carried out by placing graphite at the anode and calcined TNTs at the cathode in an electrolytic medium containing FeCl3 solution (0.1 M) as the iron source. The electrodeposition of iron was performed at various voltages, namely 2, 3, 4, 5, and 6 volts, for 15 minutes, as shown in Figure 1, to determine the effect of the deposition voltage on the formation and morphology of Fe-TNTs.

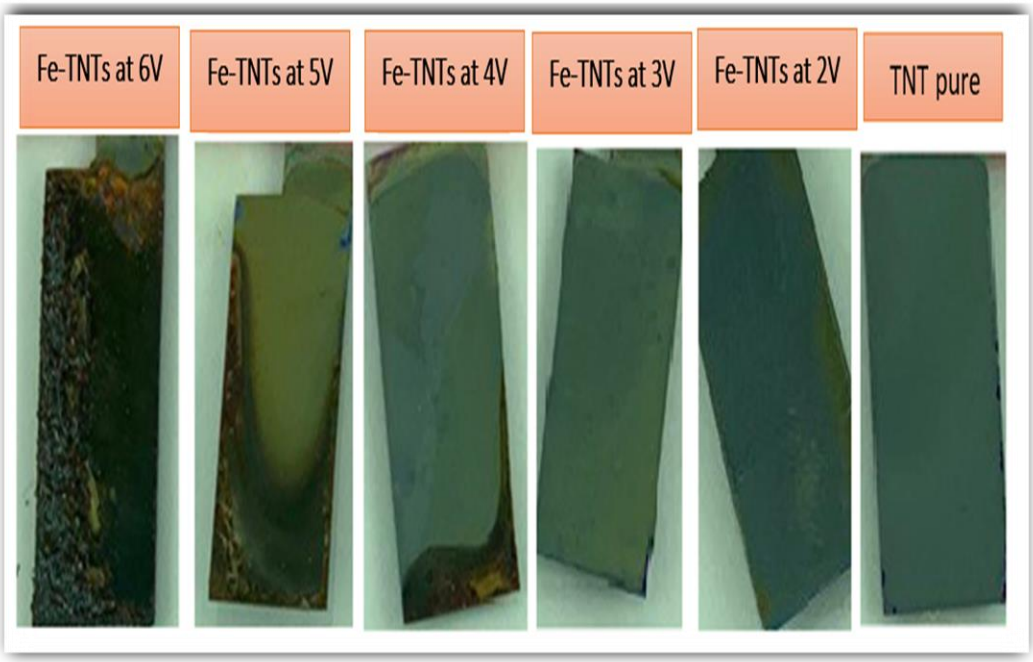

Figure 1 : The prepared samples of TNT and Fe-TNT at different voltages

2.2. Characterization of TNTs and Fe-TNTs nanotubes

The characterization of TNTs and Fe-TNTs was carried out using different techniques. The morphological properties were examined using Scanning Electron Microscopy (SEM) (Axia ChemiSEM model). Electron beam voltage of 30 kV was utilized, thus the samples were coated with metal gold at a pressure of 20 pa for 20 sec before the imaging, while the analysis of elements was run with energy dispersive spectroscopy (EDX) linked with SEM. X-ray diffractometry (XRD) (X'Pert Pro, Philips) was used to figure out the structures of TNTs and Fe-TNTAs using CuKα radiation (λ = 1.5406 Å).

2.3. Sensing system

The performance of gas sensing was measured using a sensor testing system that was homemade, as shown in Figure 2. The system comprises a 20-cm (length), 16.3-cm (diameter), and cylindrical test chamber made of stainless steel. It used a rotary pump with an inlet for gas flow and an air admittance valve for atmospheric air to evacuate the system. At the base of the chamber, a multi-pin feed-through enables electrical connections to the heater, thermocouple, and sensor electrodes. To measure the sensor's operational temperature, the GEMO DT109 PID temperature controller regulates a hot plate heater and a K-type thermocouple within the chamber to measure the operational temperature of the sensor. An APC-interfaced digital

multimeter (Vector 70C) connected to a computer is used to measure how the sensor resistance changes when air and H_2S are mixed through a flow meter and needle valve.

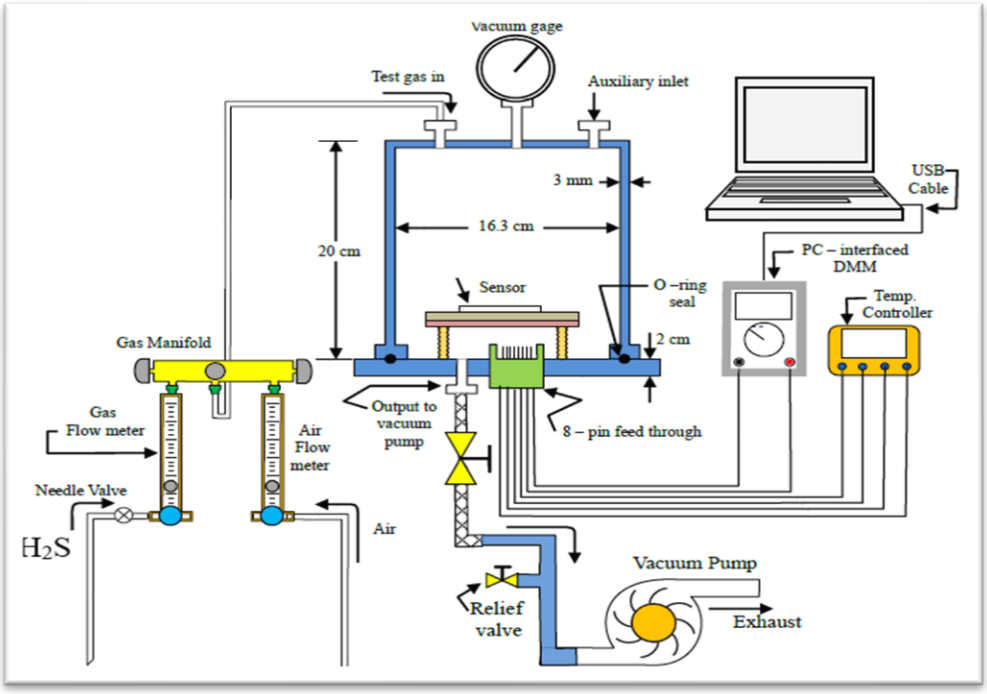

Figure 2 : Schematic diagram of the gas sensing system [32].

3. Result and discussion

3.1. Morphology of TNTs and Fe–TNTs nanostructured

The effect of doping Fe with TNTs was analysed by FESEM to examine its effect on the surface morphology of TNTs. Figure 3 depicts the FESEM images of calcined TNT and Fe-TNTs synthesized at various deposition voltages. Figure 3(a) represents the FESEM structure of the TNTs array after 1 hour of electrochemical deposition over a high surface area. The average diameter for TNTs is 85 nm, while for Fe-doped TNTs, the average diameter decreased in Figures 3(b) and 3(c) to 46.21 nm and 40.87 nm, respectively. This led to the diameter of the tubes decreasing with the increase in the deposition voltage of Fe with TNTs, whereby the increased surface area enables them to react and absorb in applications including gas sensing. As depicted in Figures 3(d) to (f), increasing Fe nanoparticles deposited on the TNTs when increasing the applied voltages. Furthermore, the aggregated Fe nanoparticles formed larger particles upon electrodeposition at more than 3 volts. Figure 3(c) illustrates the dispersion of Fe nanoparticles on the tube of TNTs at a voltage of 3.0, with some of these nanoparticles embedding into the TNTs. At 5 and 6 volts, Fe-TNT exhibited defined block-like particles that clumped together on the nanotube's top surface and obscured the underlying TNTs.

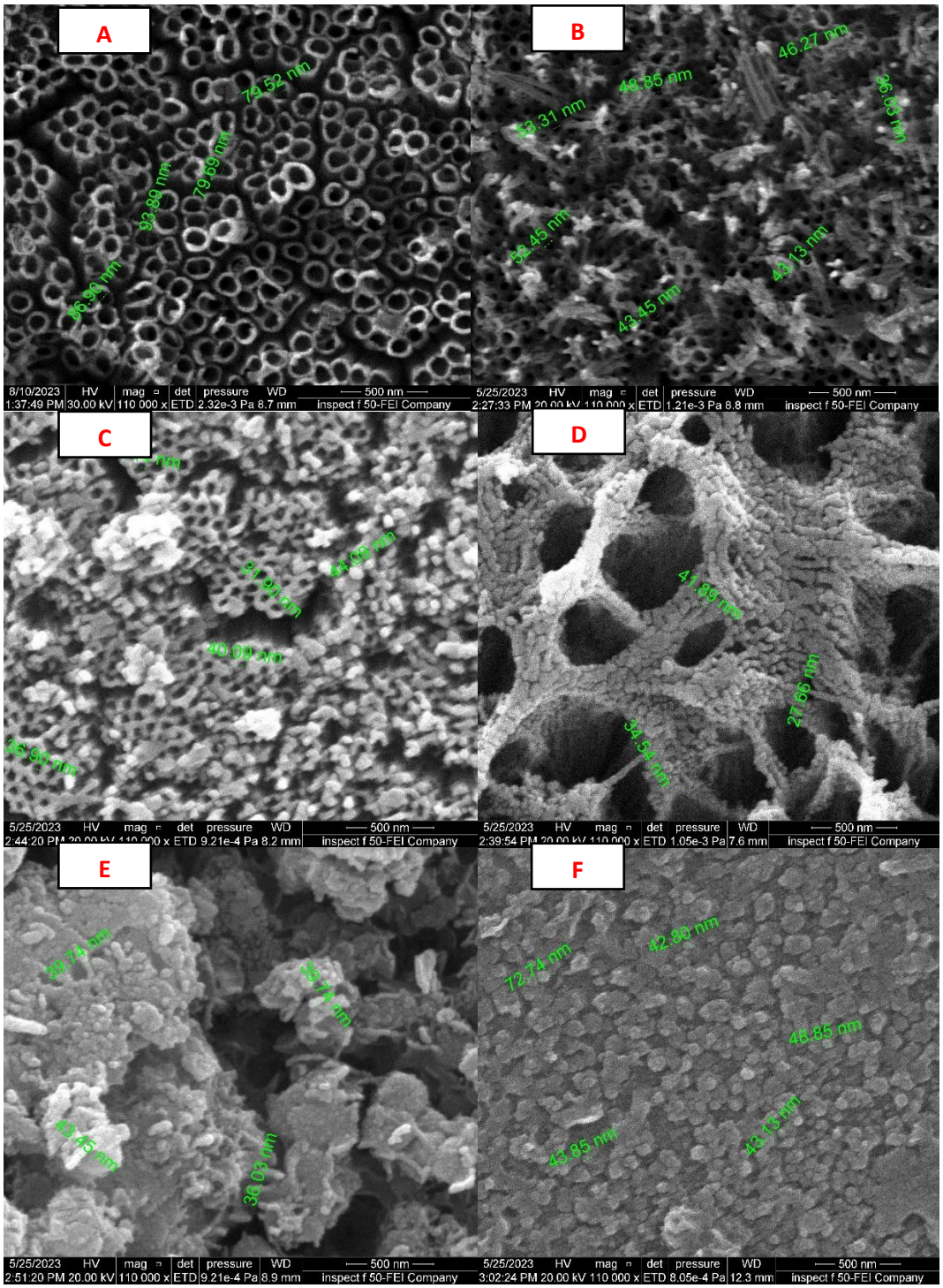

Figure 3: FESEM images of (a) TNTs and Fe-TNT films prepared at different deposition voltages, (b) 2 V, (c) 3 V, (d) 4 V, (e) 5 V, and (f) 6 V.

3.2 XRD Analysis

The phase composition and crystallinity of all produced samples are analyzed using X-ray diffractometry. Figure 4 shows that the diffraction peaks align with the anatase phase of TiO_2 (JCPDS No.00-021-1272). There were consistent peak distributions for TNTs and Fe-TNTs at 25.225 (101), 38.369 (112), 48.191 (200), 53.959 (105), 62.767 (204), and 76.022 (301), which showed signs of the anatase phase. Furthermore, the displayed Ti peaks corresponded to the Ti foil substrate and were consistent with JCPDS No.00-044-1294. However, the XRD patterns of all Fe-TNT samples lack obvious Fe diffraction peaks, with the exception of Fe-TNT at 6 volts. This could be due to its incorporation into the TiO_2 anatase structure or its dispersion within

the TiO_2 matrix. Moreover, a distinct diffraction peak was displayed for Fe (JCPDS No. 00-003-1050) due to the high quantity of Fe [33,34]. After the deposition of Fe nanoparticles, the intensity of the diffraction peaks of TNTs obviously decreased in the XRD patterns. Fe nanoparticles' coverage of TNT crystals may be the cause of this decrease. According to the literature, increasing the deposition voltage effectively deposited Fe nanoparticles onto the TNT's structure [35]. According to the work reported by Wang *et al*. in 2017, this phenomenon is consistent with their findings that the intensities of the diffraction peak (101) of Fe-TNTs become weaker than TNTs after depositing Fe in TNTs [36].

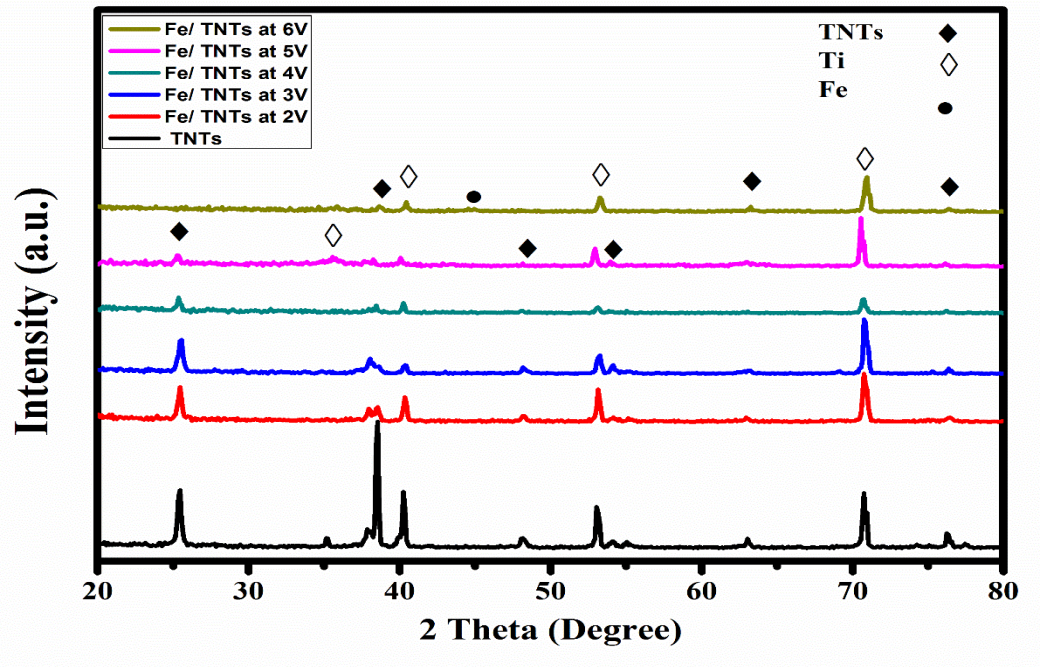

Figure 4: XRD patterns for TNTs and Fe-TNTs thin films

3.3. Elemental compositional analysis

Table 1 shows the elemental compositions of TNTs and Fe-TNTs samples prepared at different deposition voltages. As the deposition voltage increased, the amount of Fe in the Fe-TNT samples increased. Table 1 shows the results of the EDX analyses of TNTs and Fe-TNTs at 2, 3, 4, 5, and 6 volts, respectively. The measured elements include C, N, O, Ti, and Fe, individually. The results demonstrate a successful Fe deposit on the surface of TNTs. Notably, Figure 3(f) shows that Fe covered most of the TNTs' surface, which is why Fe-TNT had a much lower Ti content at 2 volts (42.5%) than TNTs (71.3%). As expected, an increase in the deposition voltage led to more Fe deposition on the TNTs. This is because a higher voltage accelerates the reaction rate, potentially leading to more Fe deposition on the TNTs' surface.

Table 1: TNTs and Fe-TNTs samples generated at various deposition voltages were analyzed using EDX to determine their elemental compositions

Samples	Atomic %				
	C	N	O	Ti	Fe
Pure TNT	4.67	3.0	21.1	71.3	Not detected
Fe-TNT at 2V	13.7	0.2	43.1	42.5	0.4
Fe-TNT at 3V	6.7	0	37.1	53.7	2.5
Fe-TNT at 4V	18.8	4.9	10.3	54.8	11.2
Fe-TNT at 5V	16.9	1.7	1.6	52.2	27.6
Fe-TNT at 6V	0.3	1.7	2.9	59.3	35.8

3.4. Gas sensor performance

Sensitivity, response, and recovery times are major concerns for gas sensing properties, primarily at low operating temperatures. It was analysed for the optimal working temperature and doping voltages (2, 3, 4, 5, and 6 volts) of the Fe-doped TNTs gas sensor, testing its responses to 450 ppm H_2S at a range of room temperature to 300 °C. At 3 volts, the Fe-TNTs showed the best response to gaseous H_2S. The response of an n-type semiconductor gas sensor to reducing gas typically depends on the difference (Ra/Rg) between the resistance in air and the resistance in the presence of gas. Figures 5-10 demonstrated an exemplary response of an oxide (n-type) across the reducing gas [37].

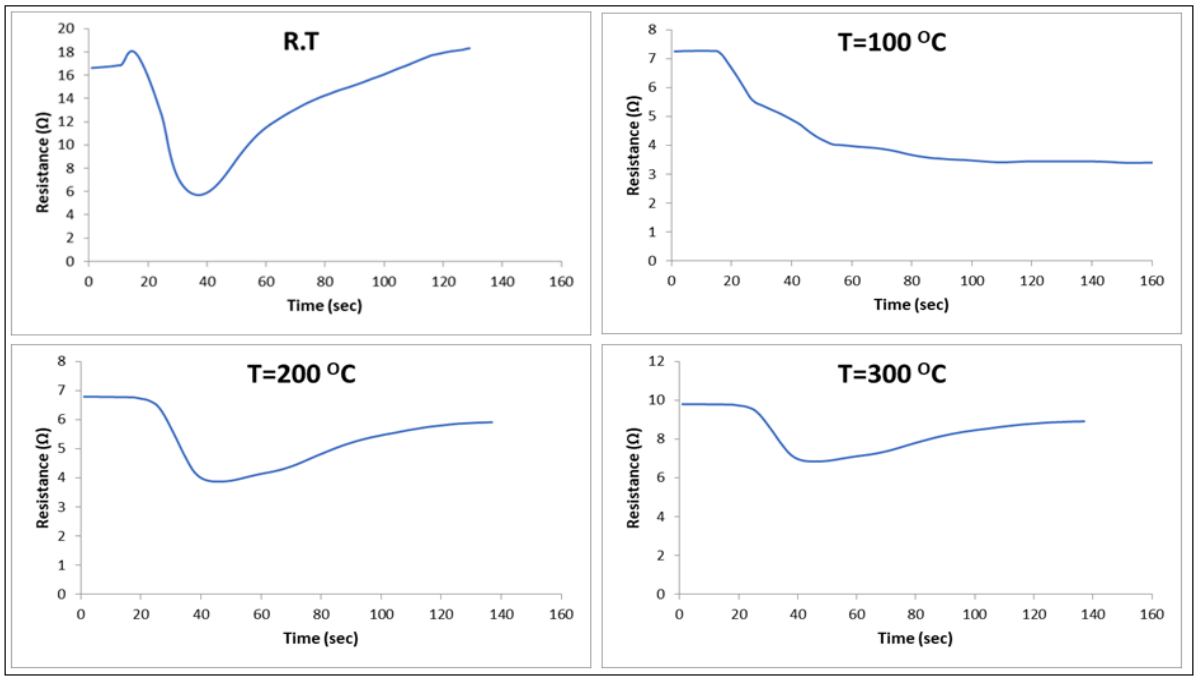

Figure 5 : Change in the resistance of TNTs prepared at 30 volts to H_2S gas at different operating temperatures

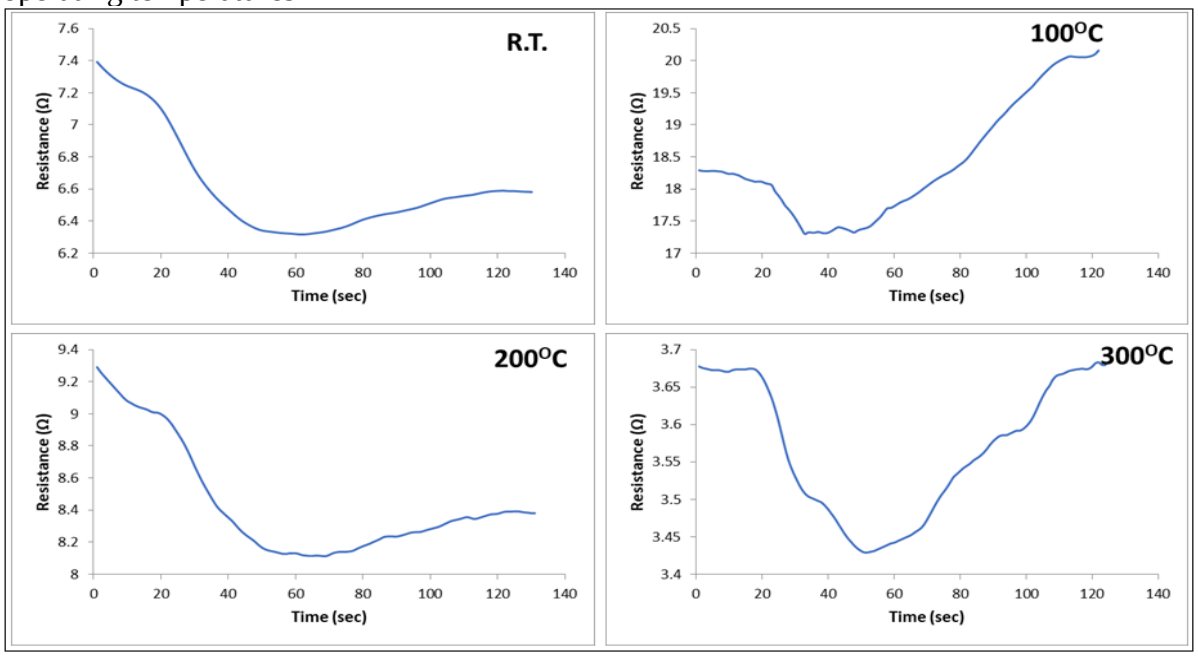

Figure 6 : Change in the resistance of Fe-TNTs prepared at 2 volts for 15 minutes to H_2S gas at different operating temperatures

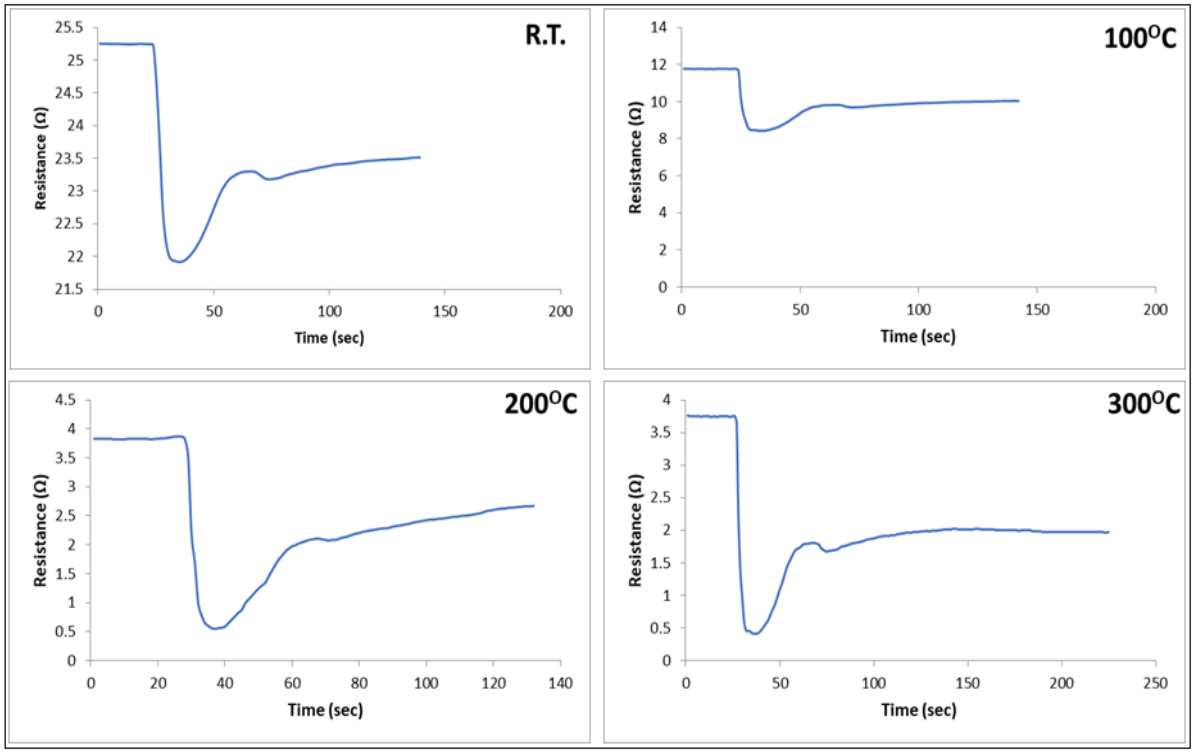

Figure 7 : Change in the resistance of Fe-TNTs prepared at 3 volts for 15 minutes to H_2S gas at different operating temperatures

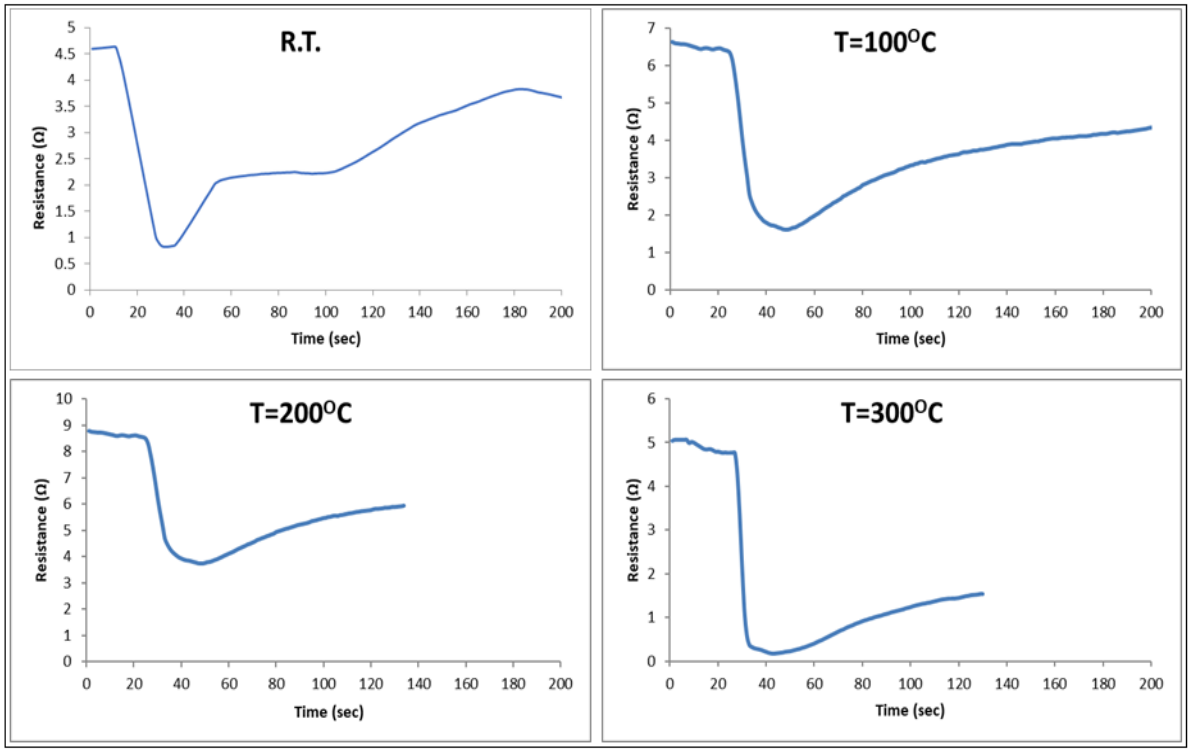

Figure 8 : Change in the resistance of Fe-TNTs prepared at 4 volts for 15 minutes to H_2S gas at different operating temperatures

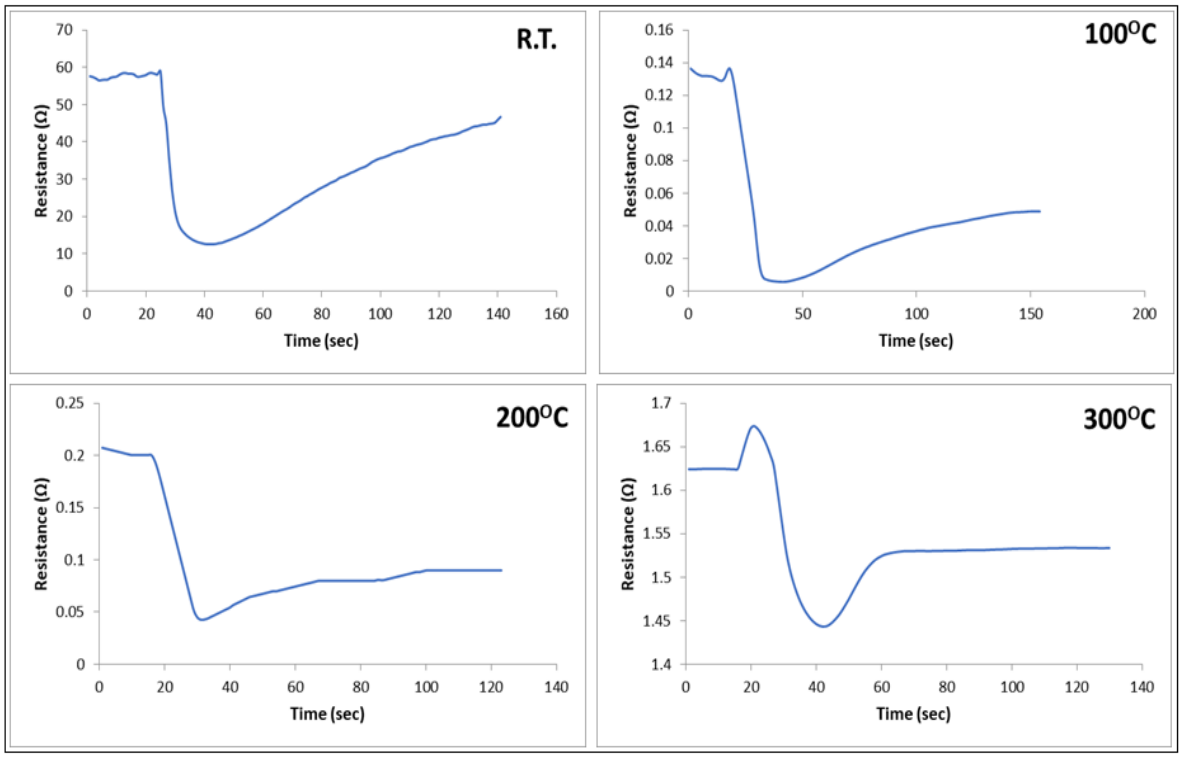

Figure 9 : Change in the resistance of Fe-TNTs prepared at 5 volts for 15 minutes to H_2S gas at different operating temperatures

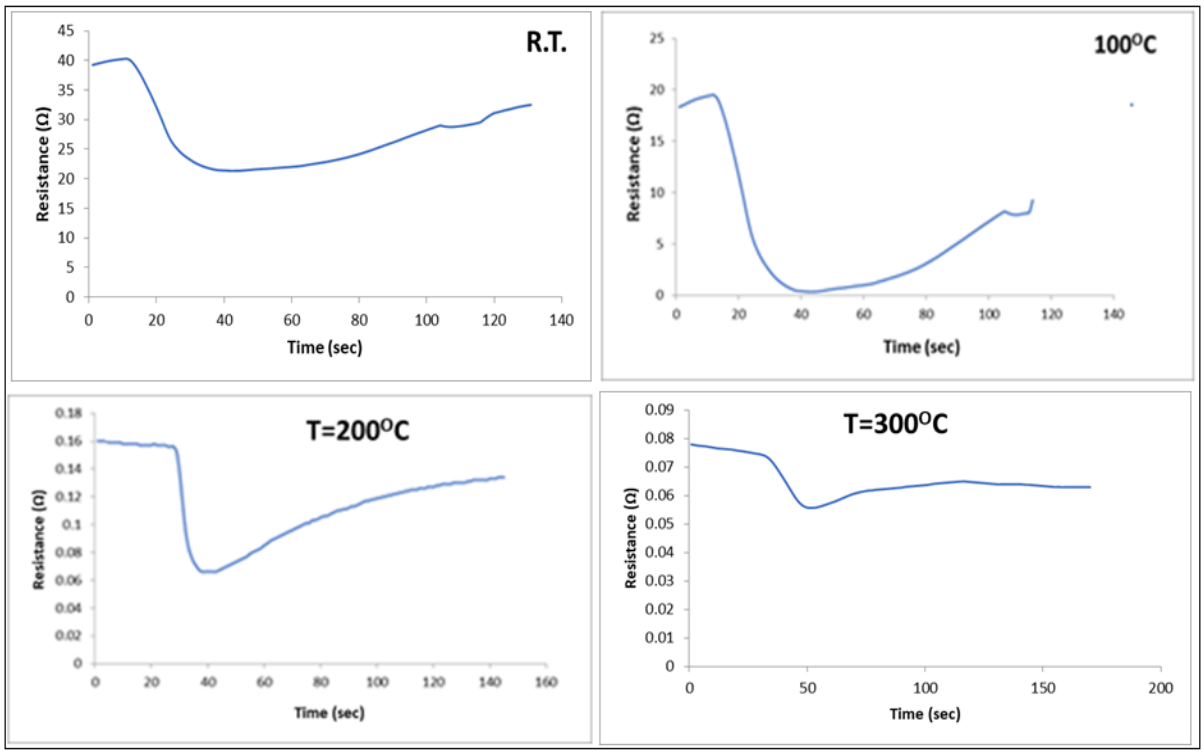

Figure 10 : Change in the resistance of Fe-TNTs prepared at 6 volts for 15 minutes to H_2S gas at different operating temperatures

The response times for TNTs and Fe-TNTs prepared at 2, 3, 4, 5, and 6 volts at low operating temperatures were 4.5, 22.5, 9, 13.5, 12.6, and 23.4 seconds, respectively. Furthermore, at operating temperature (room temperature), all TNTs and Fe-TNTs prepared as gas sensors appeared to have good H_2S sensing response times of less than 25s. As shown in Figure 11, the

recovery times for TNTs and Fe-TNTs prepared at 2, 3, 4, 5, and 6 volts at low operating temperatures were 155.6, 87.3, 153, 147.6, 74.7, and 93.6 seconds, respectively. TNTs doped with Fe might be the best nanostructure for finding gases because they have a lot of surface area [38], a fast electron transfer rate, a high ability to adsorb things [39], and a lot of holes for gas diffusion converters [40].

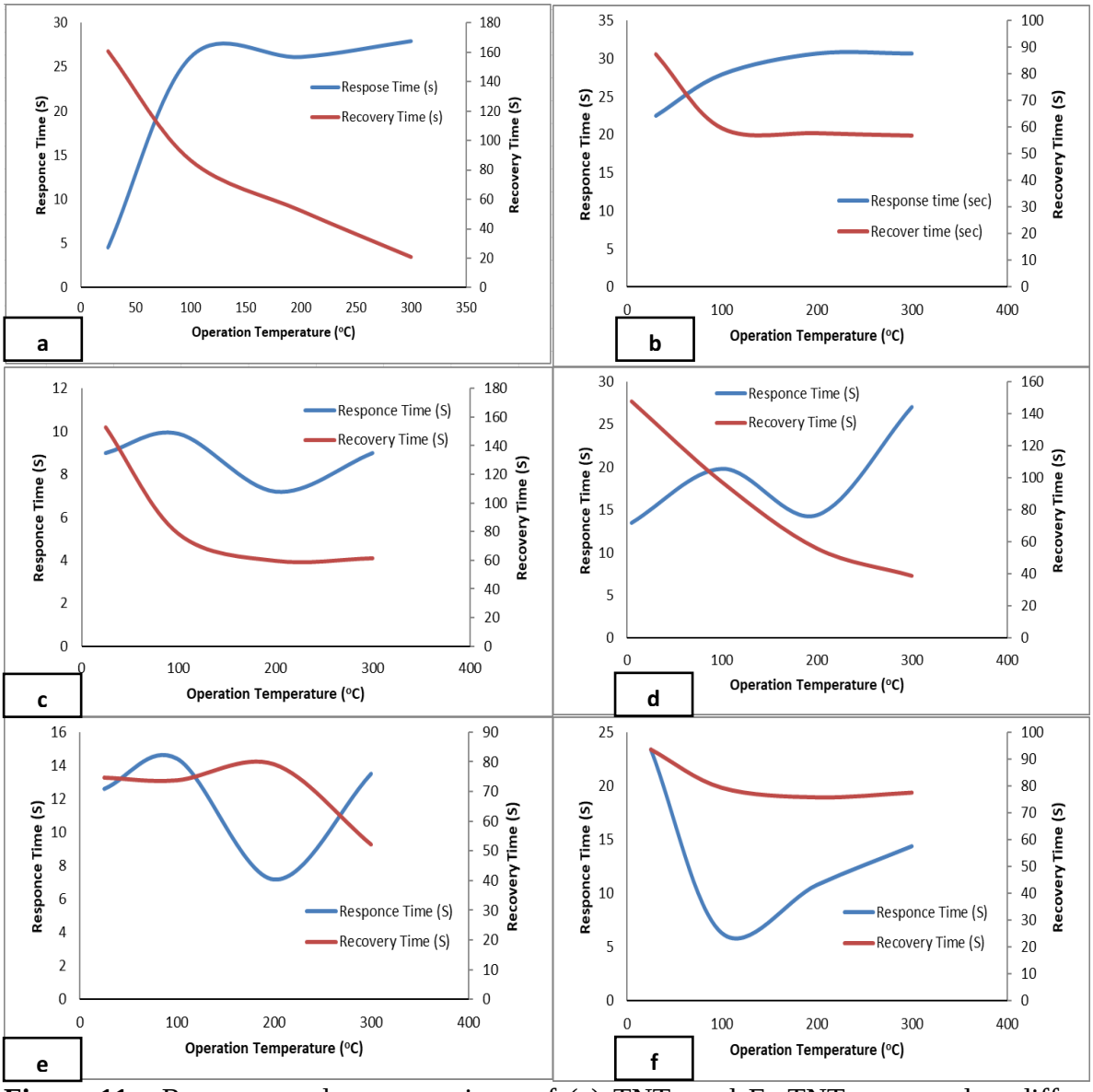

Figure 11: Response and recovery times of (a) TNTs and Fe-TNTs prepared at different deposition voltages, (b) 2 volts, (c) 3 volts, (d) 4 volts, (e) 5 volts, and (f) 6 volts

The gas sensitivity of the TNTs and Fe-TNTs sensors toward H_2S at various operation temperatures ranging from room temperature to 300 °C at a concentration of H_2S of 450 ppm. The Fe-TNTs probes exhibited a sensitivity range of approximately 65.9 to 1461.4%. At room temperature, the Fe-TNTs sensor doped at 3 volts exhibited a maximum sensitivity 38 times greater than that of TNTs. The sensitivity of the sensor primarily fluctuates with operating temperatures, as illustrated in Table 2. Therefore, the Fe-doped TNTs array film sensor is better at detecting H_2S at low temperatures than the other sensors that have been reported. This means that it responds more slowly but recovers faster when it comes to finding H_2S molecular gas [41].

Table 2: The values of sensitivity for TNTs before and after doping with Fe for different operation temperatures

T (°C)	TiO_2	Fe -TiO_2				
		2 volts	3 volts	4 volts	5 volts	6 volts
30	38.107	65.932	1461.445	520.000	338.345	91.386
100	19.736	51.102	1103.225	273.255	1525.000	26.752
200	13.220	25.825	504.687	8.028	400.000	124.285
300	7.360	7.288	715.217	1.596	20.991	34.545

The Fe-TNTs array film's gas sensing mechanism was of the surface-controlled variety, which depended on modifications in semiconductor conductance brought on by the adsorption-desorption of gas molecules on the semiconductor surface [42,43]. Fe doping in TNTs generated an electron trapping centre, aiding heat-induced electron-hole pair formation. Furthermore, Fe ions acted as intermediate energy levels, lowering the energy required for an electron transition from the valence to the conduction band. During the electron transition process, the Fe doping created an intermediate energy level that facilitated the easy passage of more electrons onto the conduction band. As a result, more oxygen species were drawn to the surface of the Fe-doped TNTs gas sensor, which effectively improved the gas sensing response. The Fe-doped TNTs sensor also had more adsorbed oxygen species on its surface than the undoped one. This made the reaction between the H_2S molecules and the adsorbed oxygen species better, which led to a shorter response time and a longer recovery time [42].

4. Conclusion

This work represents a feasible way of depositing Fe on TiO_2 nanotube arrays using an electrochemical method. The morphology of Fe-TNT nanotubes was preserved when the deposition voltage was 2-6 volts in 0.1 M $FeCl_3$. Several techniques for characterizing materials, such as XRD, FESEM, and EDX, helped add Fe to TNTs, as shown by the gas sensor test. The response of the gas sensor with 450 ppm H_2S at room temperature is about 9s for Fe-TNTs at 3 volts, while the recovery time is about 153s for the same sample. We have successfully prepared gas sensors (Fe-TNTs) that operate at room temperature with an ultra-high sensitivity of 1461.44%, compared to 38.107% for TNTs. This work proposes a strategy to enhance the execution of TiO_2 nanotube-based gas sensors by modifying nanoparticle loading.

Acknowledgments

Special thanks are extended to the Department of Chemistry, College of Science for Women, University of Baghdad, Baghdad, Iraq.

Conflict of interest

The authors declare that they have no known financial interests or personal relationships that could have influenced the study they reported in this paper.

References

[1] P. S. Jagannath, A. V. Patil, C. G. Dighavkar, K. S. Thakare, R. Y. Borase, S. J. Nandre, N. G. Deshpande, and R. R. Ahire, "Semiconductor metal oxide compounds-based gas sensors: A literature review", *Frontiers of Materials Science*, vol. 9, no. 1, pp. 14-37, 2015.

[2] N. A. Samsudin, Z. Zainal, H. N. Lim, Y. Sulaiman, S. K. Chang, Y. C. Lim, and W. N. Amin, "Capacitive performance of vertically aligned reduced titania nanotubes coated with Mn_2O_3 by reverse pulse electrodeposition", *RSC Advances*, vol. 8, no. 41, pp. 23040-23047, 2018.

[3] A. K. Ayal, Y. C. Lim, and A. M. Farhan, "Sensitization of Mn with CdS nanoparticles *via*

electrochemical deposition technique for photocurrent enhancement of nanomaterial's-sensitized photoelectrochemical cells", *Research on Chemical Intermediates*, vol. 44, no. 12, pp. 7231-7240, 2018.

[4] A. K. Ayal, "Enhanced photocurrent of titania nanotube photoelectrode decorated with CdS nanoparticles", *Baghdad Science Journal*, vol. 15, no. 1, pp. 57-62, 2018.

[5] L. B. Tasyurek, E. Isik, I. Isik, and N. Kilinc, "Enhancing the performance of TiO_2 nanotube-based hydrogen sensors through crystal structure and metal electrode", *International Journal of Hydrogen Energy*, vol. 54, no. 7, pp. 678-690, 2024.

[6] E. Isik, L. B. Tasyurek, E. Tosun, and N. Kilinc, "Enhancing high sensitive hydrogen detection of Bi_2O_3 nanoparticle decorated TiO_2 nanotubes", *Materials Chemistry and Physics*, vol. 311, no. 1, pp. 128535-128549, 2024.

[7] P. Dwivedi, N. Chauhan, P. Vivekanandan, S. Das, D. S. Kumar, and S. Dhanekar, "Scalable fabrication of prototype sensor for selective and sub-ppm level ethanol sensing based on TiO_2 nanotubes decorated porous silicon", *Sensors and Actuators B: Chemical*, vol. 249, no. October, pp. 602-610, 2017.

[8] A. M. A. Al-Sammarraie, H. I. Jaafer, and H. H. Hamdan, "Study of the effect of NH_4F concentration on the structure of electrochemically prepared TiO_2 nanotubes", *Iraqi Journal of Science*, vol. 53, no. 2, pp. 827-831, 2012.

[9] S. Zampolli, I. Elmi, J. S. Urmann, S. Nicoletti, L. Dori, and G. C. Cardinali, "Selectivity enhancement of metal oxide gas sensors using a micromachined gas chromatographic column", *Sensors and Actuators B: Chemical*, vol. 105, no. 2, pp. 400-406, 2005.

[10] D. D. Lee and D. K. Lee, "Environmental gas sensors", *IEEE Sensors Journal*, vol. 1, no. 3, pp. 214-224, 2001.

[11] D. L. Wang, A. T. Chen, Q. F. Zhang, and G. Z. Cao, "Room-temperature chem-iresistive effect of TiO_2 nanowires to nitroaromatic and nitroamine explosives", *IEEE Sensors Journal*, vol. 11, no. 6, pp. 1352-1358, 2011.

[12] Z. Bielecki, J. Janucki, A. Kawalec, J. Mikolajczyk, N. Palka, M. Pasternak, T. Pustelny, T. Stecewicz, and J. Wojtas, "Sensors and systems for the detection of explosive devices-anoverview", *Metrology and Measurement Systems*, vol. 19, no. 1, pp. 3-28, 2012.

[13] B. S. Fisher, K. Woffenden, A. Matysek, M. Ford, and V. Tulpulé, "Alternatives to the Kyoto protocol: A new climate policy framework", *International Review for Environmental Strategies*, vol. 5, no. 1, pp. 179-197, 2004.

[14] M. Kastek, T. Piątkowski, and P. Trzaskawka, "Infrared imaging fourier transform spectrometer as the stand-off gas detection system", *Metrology and Measurement Systems*, vol. 18, no. 4, pp. 607-620, 2011.

[15] U. Yaqoob and I. Y. Mohammad, "Chemical gas sensors: Recent developments, challenges, and the potential of machine learning - A review", *Sensors*, vol. 21, no. 8, Article no. 2877 (40 pages), 2021.

[16] N. M. Shaalan, A. Faheem, O. Saber, and S. Kumar, "Gases in food production and monitoring: Recent advances in target chemiresistive gas sensors", *Chemosensors*, vol. 10, no. 8, Article no. 338 (20 pages), 2022.

[17] H. Xin, W. Ming, A. Zhimin, B. Lai, Y. Zhou, A. Taicheng, and S. Wang, "Metal-organic frameworks derived C/TiO_2 for visible light photocatalysis: Simple synthesis and contribution of carbon species", *Journal of Hazardous Materials*, vol. 403, no. February, Article no. 124048, 2021.

[18] L. Tianpeng, Y. Rui, X. Zhang, J. Shi, X. Wang, Y. Wang, J. Yang, and Q. Zhang, "Anatase TiO_2 nanorod arrays as high-performance electron transport layers for perovskite solar cells", *Journal of Alloys and Compounds*, vol. 849, no. December, Article no. 156629, 2020.

[19] P. V. Shinde and C. S. Rout, "Magnetic gas sensing: Working principles and recent developments", *Nanoscale Advances*, vol. 3, no. 6, pp. 1551-1568, 2021.

[20] Y. J. Choi, Z. Seeley, A. Bandyopadhyay, S. Bose, and S. A. Akbar, "Aluminum-doped TiO_2 nano-powders for gas sensors", *Sensors and Actuators B: Chemical*, vol. 124, no. 1, pp. 111-117, 2007.

[21] W. D. Zhang and W. H. Zhang, "Carbon nanotubes as active components for gas sensors", Journal of Sensors", vol. 2009, no. Special Issue, pp. 1-16, 2009.

[22] M. M. Alalousi, J. M. Rzaij, I. M. Ibrahim, A. Ramizy, and M. H. Eisa, "Sensing enhancement of gold nanoparticles doped-TiO_2 thin films as H_2S gas sensor", *Nano Hybrids and Composites*, vol. 35, no. May, pp. 1-10, 2022.

[23] A. M. Taurino, S. Capone, P. Siciliano, T. Toccoli, A. Boschetti, L. Guerini, and S. Iannotta, "Nanostructured TiO_2 thin films prepared by supersonic beams and their application in a sensor array for the discrimination of VOC", *Sensors and Actuators B: Chemical*, vol. 92, no. 3 pp. 292-302, 2003.

[24] W. Chengxiang, L. Yin, L. Zhang, D. Xiang, and R. Gao, "Metal oxide gas sensors: sensitivity and influencing factors", *Sensors*, vol. 10, no. 3, pp. 2088-2106, 2010.

[25] S. K. Tripathi, R. Kaur, and M. Rani, "Oxide nanomaterials and their applications as a memristor", *Solid State Phenomena*, vol. 222, no. February, pp. 67-97, 2015.

[26] R. S. Khaleel and M. S. Hashim, "Fabrication of TiO_2 sensor using rapid breakdown anodization method to measure pressure, humidity and sense gases at room temperature", *Iraqi Journal of Science*, vol. 60, no. 8, pp. 1694-1703, 2019.

[27] E. Ehsan, A. S. Noce, and F. Taghipour, "The effect of radiation parameters on the performance of photo-activated gas sensors", *Journal of Photochemistry and Photobiology A: Chemistry*, vol. 374, no. April, pp. 95-105, 2019.

[28] M. Shuangfeng, J. Jia, Y. Tian, L. Cao, S. Shi, X. Li, and X. Wang, "Improved H_2S sensing properties of Ag/TiO_2 nanofibers", *Ceramics International*, vol. 42, no. 1, pp. 2041-2044, 2016.

[29] C. Prapti and S. Mishra, "Effect of CuO as a dopant in TiO_2 on ammonia and hydrogen sulphide sensing at room temperature", *Measurement*, vol. 90, no. August, pp. 468-474, 2016.

[30] T. J. Awaid, A. K. Ayal, A. M. Farhan, M. S. Sando, and L.Y. Chin, "Effect of electrolyte composition on structural and photoelectrochemical properties of titanium dioxide nanotube arrays synthesized by anodization technique", *Baghdad Science Journal*, vol. 17, no. 4, pp. 1183-1183, 2020.

[31] V. Baiju, N. M. Dimitrijevic, T. Rajh, and K. Gray, "Effect of calcination temperature on the photocatalytic reduction and oxidation processes of hydrothermally synthesized titania nanotubes", *The Journal of Physical Chemistry C*, vol. 114, no. 30, pp. 12994-13002, 2010.

[32] M. H. Suhail, A. A. Ramadan, S. B. Aziz, and O. G. Abdullah, "Chemical surface treatment with toluene to enhance sensitivity of NO_2 gas sensors based on $CuPcTs/Alq_3$ thin films", *Journal of Science: Advanced Materials and Devices*, vol. 2, no. 3, pp. 301-308, 2017.

[33] L. Y. Chin, Z. Zainal, Z. Khusaimi, and S. S. Ismail, "Electrochemical synthesis of ordered titania nanotubes in mixture of ethylene glycol and glycerol electrolyte", *Malaysian Journal of Analytical Sciences*," vol. 20, no. 2, pp. 373-381, 2016.

[34] M. Li, C. Zou, F. Liang, E. Hou, and J. Lin, "Preparation and gas-sensing performance under photoactivation of TiO_2 nanotubes/carbon nanotubes/ZnS quantum dots gas-sensitive materials", *Materials Today Communications*, vol. 36, no. August, Article no. 106487, 2023.

[35] C. H. Chen, Y. P. Peng, M. H. Lin, K. L. Chang, Y. C. Lin, and J. Sun, "Iron modified titanate nanotube arrays for photoelectrochemical removal of E. coli", *Nanomaterials*, vol. 11, no. 8, Article no. 1944 (17 pages), 2021.

[36] Q. Wang, J. Rencheng, M. Zhang, and S. Gao, "Solvothermal preparation of Fe-doped TiO_2 nanotube arrays for enhancement in visible light induced photoelectrochemical performance", *Journal of Alloys and Compounds*, vol. 690, no. January, pp. 139-144, 2017.

[37] A. Dey, "Semiconductor metal oxide gas sensors: A review," *Materials Science and Engineering: B*, vol. 229, no. March, pp. 206-217, 2018.

[38] J. Tang, X. Zhang, S. Xiao, and F. Zeng, "Application of TiO_2 nanotubes gas sensors in online monitoring of SF6 insulated equipment", *Nanomaterials Based Gas Sensors for SF6 Decomposition* Components Detection, 2017.

[39] B. Santhosh, Y. Umehara, K. Higashimine, R. Badam, R. Vedarajan, and N. Matsumi, "Ultrafast electrochemical deposition of core shell metal nanoparticles on TiO_2 nanotubes for electrocatalytic applications", *Materials Research Express*, vol. 5, no. 11, Article no. 115016, 2018.

[40] N. D. Chinh, K. Chunjoong, and K. Dojin, "UV-light-activated H_2S gas sensing by a TiO_2 nanoparticulate thin film at room temperature", *Journal of Alloys and Compounds*, vol. 778, no. 25 March, pp. 247-255, 2017.

[41] X. Tong, W. Shen, X. Zhang, J. P. Corriou, and X. Hongxia, "Synthesis and density functional theory study of free-standing Fe-doped TiO_2 nanotube array film for H_2S gas sensing properties at low temperature", *Journal of Alloys and Compounds*, vol. 832, no. August, Article no. 155015 (11 pages), pp.1-12, 2020.

[42] X. Tong, W. Shen, and X. Chen, "Enhanced H_2S sensing performance of cobalt doped free-standing

TiO_2 nanotube array film and theoretical simulation based on density functional theory", *Applied Surface Science*, vol. 469, no. March, pp. 414-422, 2019.

[43] X. Tong, X. Zhang, H. Wang, Z. Lin, H. Xi, and J. Li, "Effect of humidity on the sensitivity of an ion-doped TiO_2 nanotube-based gas sensor to H_2S and its mechanism via density functional theory", *Journal of Electronic Materials*, vol. 51, no. 9, pp. 5440-5453, 2022.